

Inter-laboratory Comparison between Particle and Bacterial Filtration Efficiencies of Medical Face Masks in the COVID-19 Context

Axel Fouqueau^{1*}, Jérémie Pourchez², Lara Leclerc², Aurélien Peyron², Yoann Montigaud², Paul Verhoeven^{3,4}, Tatiana Macé¹, Alexandre Bescond¹, Dominique Thomas⁵, Augustin Charvet⁵, Mathieu Ghijssels⁶, Pauline Hars⁶, Franck Polyn⁶, François Gaie-Levrel¹

¹ Laboratoire national de métrologie et d'essais (LNE), 75015 Paris, France

² Mines Saint-Etienne, Univ Lyon, Univ Jean Monnet, INSERM, U 1059 Sainbiose, Centre CIS, F-42023 Saint-Etienne, France

³ CIRI (Centre International de recherche en Infectiologie), INSERM U111 – CNRS UMR 5308 – ENS de Lyon – UCB Lyon 1, Equipe GIMAP, Université Jean-Monnet, Saint-Etienne, France

⁴ Laboratory of Infectious Agents and Hygiene, University Hospital of Saint-Etienne, France

⁵ Université de Lorraine, CNRS, LRGP, F-54000 Nancy, France

⁶ HeX Lab, 145 Porte des bâtisseurs, B7730 Estaimpuis, Belgium

ABSTRACT

Severe acute respiratory syndrome coronavirus-2 (SARS-CoV-2) transmission lead to the recommendation of mask wearing during the pandemic COVID-19. Bacterial filtration efficiency (BFE) measurements are used to measure the efficiency of medical face masks in preventing the spread of bioaerosols. Even though these measurements are simple, BFE testing still raise several scientific questions. This paper presents an inter-laboratory comparison between Bacterial Filtration Efficiency (BFE) and Particle Filtration Efficiency (PFE), in order to better understand and establish an overview of both ways for testing surgical masks. Filtration efficiency of six commercial surgical masks have been measured using such experimental methods, i.e., the BFE and the PFE using 3 µm particles initially developed for community face covering testing. The fractional filtration efficiencies have been measured and compared in order to explain the differences. Recommendations for improving associated EN14683:2019+AC standard are also proposed according to the results.

Keywords: Filtration efficiency, Inert aerosol, Biologic aerosol, Medical face masks

OPEN ACCESS

Received: June 21, 2022

Revised: December 2, 2022

Accepted: December 13, 2022

* **Corresponding Author:**


axel.fouqueau@lne.fr

Publisher:

Taiwan Association for Aerosol
Research

ISSN: 1680-8584 print

ISSN: 2071-1409 online

 **Copyright:** The Author's institution. This is an open access article distributed under the terms of the [Creative Commons Attribution License \(CC BY 4.0\)](https://creativecommons.org/licenses/by/4.0/), which permits unrestricted use, distribution, and reproduction in any medium, provided the original author and source are cited.

1 INTRODUCTION

Since 2019 and the appearance of the severe acute respiratory syndrome coronavirus-2 (SARS-CoV-2), the World Health Organization (WHO) has officially declared the global outbreak of coronavirus disease 2019 (COVID-19) as a pandemic (WHO, 2020). This virus has infected more than 460 million people worldwide and may have caused more than 6,340,000 deaths (Worldometer, 2022). Such respiratory viruses are potentially transmitted by three routes simultaneously, namely airborne, contact and droplet (Galbadage *et al.*, 2020; Hobday and Dancer, 2013; Jones and Brosseau, 2015; Tellier *et al.*, 2019). Airborne transmissions include aerosol and droplet emissions during sneezing, coughing, breathing or talking. These activities can generate both sub- and supermicron particles (Nicas *et al.*, 2005).

The role and spatial extent of these three modes of transmission is still a matter of uncertainty in certain respiratory diseases, including COVID-19 (Asadi *et al.*, 2020a; Bourouiba, 2020; Dancer *et al.*, 2020; Peters *et al.*, 2020). Bahl *et al.* (2020) highlighted the evidence for the horizontal



distance that droplets travel in their review: eight studies showed that droplets with a size of 10–100 μm travel more than 2 meters, with an exhalation/cough velocity between 10 and 50 m s^{-1} , and in some cases up to 8 meters due to evaporation of the smaller droplets. Large droplets with a diameter and initial velocity of more than 500 μm and 5 m s^{-1} , respectively, can also travel more than 2 metres (Wang *et al.*, 2020). Ng *et al.* (2021) have shown that respiratory droplets (with a diameter of several tens of micrometres) can move further away in cold and humid weather due to the protection provided by the supersaturated vapour field.

In order to separate droplets from aerosols in terms of their physical behaviour, a size threshold of 100 μm was set. Nevertheless, droplets released during expiration are initially assumed to have an effective average diameter of 5 μm . This diameter rapidly shrinks in ambient air to aerosol particles with a diameter of 1 μm (Cheng *et al.*, 2020b; Johnson *et al.*, 2011). The fact that the droplet diameter usually remains smaller than 5 μm actually seems to be subject to consensus (Asadi *et al.*, 2020b; Johnson *et al.*, 2011). Viruses have been shown to be associated with droplets of 2.5 μm and smaller, and they can remain airborne for more than 2 hours (Liu *et al.*, 2020). In other studies, SARS-CoV-2 has been detected in aerosols in the size range of 1–4 micrometres (Birgand *et al.*, 2020; Chia *et al.*, 2020).

Assuming that both droplet and aerosol transmission contribute to different proportions of SARS-CoV-2 transmission, reduction of droplets at the source is required to prevent transmission (Eiche and Kuster, 2020). In addition, some studies found viral RNA in air sampling (Chia *et al.*, 2020; Guo *et al.*, 2020; Santarpia *et al.*, 2020) whereas others did not (Cheng *et al.*, 2020a; Cheng *et al.*, 2020b; Chia *et al.*, 2020; Wong *et al.*, 2020; Faridi *et al.*, 2020; Ong *et al.*, 2020). Consequently, the wearing of face masks has been suggested as a means of containing disease transmission, particularly in healthcare settings. In this context, surgical masks were instrumental in the COVID-19 pandemic.

The mask shortage in the early phase of pandemic showed that it was necessary to increase both the production and the availability of face masks and also increase the number of specialist centres able to conduct regulatory tests to assess mask performance. A medical face mask (MFM) is a medical device. It is manufactured according to a standard (EN14683+ACI, CEN, 2019b; ASTM F2100-19, ASTM International, 2019) and is designed to protect the environment from the spreading of droplets by the wearer. Indeed, surgical masks have been shown to reduce the spread of viruses delivered by an infected wearer by up to ~67–75% and, in the case of seasonal coronavirus, by as much as 100% (Milton *et al.*, 2013; Leung *et al.*, 2020). When an infectious person wears a face mask, the size of the exhaled plume is also reduced, which helps to reduce the risk of inhalation exposure. It can also protect the wearer from droplets coming from a person who stands directly in front. Nevertheless, it does not always protect against inhalation of very small airborne particles that can potentially carry the virus. Among other characteristics of MFMs, the EN14683:2019+AC standard describes the performance requirements and test methods for MFMs in order to limit the transmission of infectious agents from staff to patients in surgical procedures (and other similar medical facilities). In Europe, a disposable MFM must be labelled with a reference to this standard and the type of mask it is intended to be. Four performance criteria are intended to confirm the quality of the MFM: Breathability, splash protection, microbial purity and bacterial filtration efficiency (BFE). BFE is a crucial parameter for determining MFM performance. There are three types of surgical masks defined in the standard: (i) Type I: BFE $\geq 95\%$, (ii) Type II: BFE $\geq 98\%$ and (iii) Type IIR: BFE $\geq 98\%$ and splash-proof. Type I MFMs are used at least for patients to reduce spreading airborne pathogens, particularly in epidemic/pandemic situations. Type II MFM is designed to be used by medical professionals in a medical facility.

The EN14683:2019+AC standard involves a *Staphylococcus aureus* aerosol characterized by a mean size of 3.0 $\mu\text{m} \pm 0.3 \mu\text{m}$ with a biological culture downstream of the MFM tested as a function of aerodynamic diameters. Other standards and guidance documents for face masks (EN149+A1, CEN, 2009; EN13274-7, CEN, 2019a) include measurement of particle filtration efficiency (PFE) using inert aerosol. The assessment of Community Face Masks (NSAI, 2020) requires the use of 3 μm particles (3 μm PFE) to characterize filtration efficiency. Several studies measured various inert and bioaerosol penetrations and showed variations between 10 and 90% of efficiency for filter media used in surgical masks (Weber *et al.*, 1993; Chen *et al.*, 1994; McCullough *et al.*, 1997).

Therefore, the purpose of this study is to compare the BFE with the 3 μm -PFE to verify the agreement and to provide an overview of the two assessment methods of MFM. BFE and 3 μm -



PFE of six commercial surgical mask samples were measured, and a comparison in terms of fractional efficiencies is presented to explain the observed differences and to highlight necessary recommendations to improve the associated EN14683:2019+AC standard.

2 MATERIALS AND METHODS

In this comparison, two laboratories were involved by measuring 3 μm -PFE (Lab. 1 and Lab. 2) and two other by measuring BFE (Lab. 3 and Lab. 4). Six samples of commercial MFM were chosen to be compared. For a confidentiality purpose, the names of tested masks will not be published.

2.1 Particle Filtration Efficiency at 3 μm (3 μm -PFE)

According to the CWA 17553:2020 specifications (NSAI, 2020), a filtration velocity of $6 \pm 1 \text{ cm s}^{-1}$ is used. It is calculated from human expelled air flowrate and mean community face coverings filtration surface. Nevertheless, in order to compare BFE with 3 μm -PFE, the PFE filtration velocity has been fixed at 10.1 cm s^{-1} for this study, calculated using a flow rate of 28.3 L min^{-1} and an effective filtration surface of 46.5 cm^2 . Indeed, this effective filtration surface represents the real available surface in the involved filter holders. PFE is therefore defined as:

$$PFE(d_p) = 1 - \frac{C_{N,down}(d_p)}{C_{N,up}(d_p)} \quad (1)$$

where $C_{N,down}$ and $C_{N,up}$ are the particle number concentrations of the MFM sample measured at 3 μm (3 μm -PNC) downstream and upstream, respectively.

2.1.1 Lab.1 experimental set-up

Fig. 1 presents the test bench used by Lab. 1. A Polystyrene Latex (PSL) aerosol, composed of monodisperse particles characterized by diameter of $2.8 \mu\text{m} \pm 0.14 \mu\text{m}$, is produced by a nebulizer (AGK 2000, PALAS). Two separate aerosol transport ducts are used to measure the filtration efficiency. One is associated with a 47 mm filter holder (effective filtration surface of 10.7 cm^2). Line 1 is composed of a filter holder whereas line 2 is not. The particle concentration at the 3 μm size bins are measured by an Aerodynamic Particle Size spectrometer (APS, TSI Inc., model 3321).

For the 3 μm -PFE measurements, 3 μm -PNC measured from the APS size distribution in line 2 (empty line), corresponds to the upstream concentration ($C_{N,up}$). Then, 3 μm -PNC measured in line 1, corresponds to the downstream PNC ($C_{N,down}$). Finally, one APS size distribution is measured in line 2, corresponding to the second upstream concentration ($C_{N,up,2}$), in order to verify the stability of the concentration. An averaged 3 μm -PFE is then calculated from five tests performed

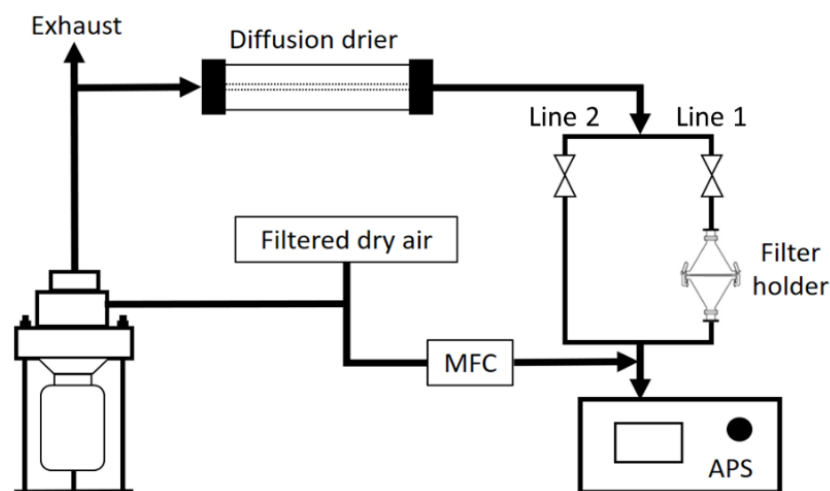
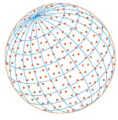


Fig. 1. Experimental test bench used by Lab. 1 for 3 μm -PFE measurements.



on MFM samples. The associated uncertainty $u(E_N(d_p))$ is calculated using the following formula:

$$u(E_N(d_p)) = \sqrt{\frac{100C_{N,down}(d_p)}{C_{N,up}(d_p)^2} \sigma(C_{N,up}(d_p)) + \frac{100}{C_{N,up}(d_p)^2} \sigma(C_{N,down}(d_p))} \quad (2)$$

where, $\sigma(C_{N,up}(d_p))$ and $\sigma(C_{N,down}(d_p))$ are the standard deviations associated with the mean values of upstream and downstream concentration respectively. The global associated error is calculated as the quadratic sum of the maximum value of $u(E_N(d_p))$ and the standard deviation on the five values measured with the five tests.

2.1.2 Lab.2 experimental set-up

The experimental test bench used by Lab. 2 is presented in Fig. 2. DEHS (di-ethyl-hexylsebacate) aerosol is generated by an AGK 2000 Palas nebulizer and diluted with compressed air. After dilution, the DEHS particle number size distribution is measured upstream of the MFM sample with an Aerodynamic Particle Sizer TSI 3321, and is characterized by a mean diameter around $0.85 \mu\text{m}$. For MFM $3 \mu\text{m}$ -PFE tests, a sample is placed in a filter holder with a filtration surface of 28.3 cm^2 , leading to a 10.1 cm s^{-1} filtration velocity. A $3 \mu\text{m}$ -PFE measurement is done by a series of seven measurements conducted successively upstream and downstream of the sample. In order to purge and stabilize the particle concentration in the sampling lines, a sampling of 30 seconds is performed before each measurement. These seven successive counts allow obtaining three efficiency results for the same material sample (repeatability test). Efficiency measurements at the $3\text{-}\mu\text{m}$ size bin were conducted on three or four MFM samples (reproducibility test).

It is important to mention that, considering the concentration of the DEHS aerosol, the droplets do not discharge the filter during the experiment. Measuring three comparable efficiencies associated to the previously described protocol, tends to prove that a discharge phenomenon does not occur.

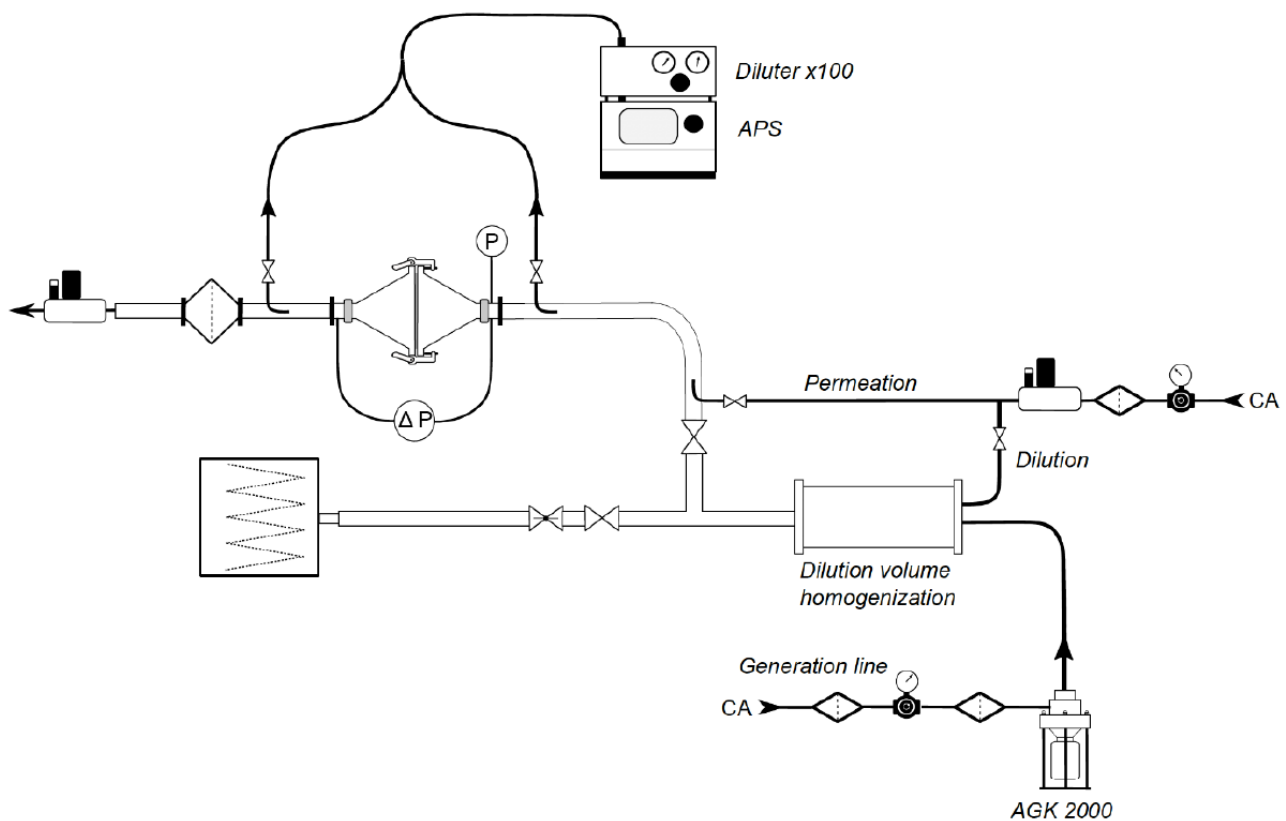


Fig. 2. Experimental test bench used by Lab. 2 for $3 \mu\text{m}$ -PFE measurements (from Bourrous et al., 2021).

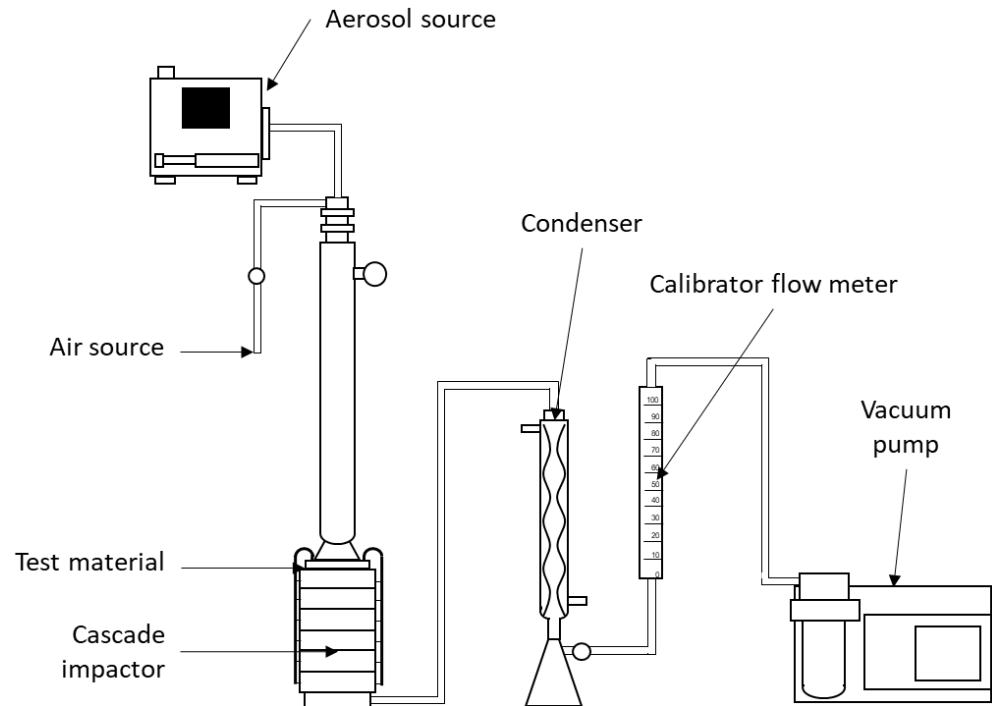


Fig. 3. Experimental setup used for the BFE measurements according to the EN 14683:2019 standard.

2.2 Bacterial Filtration Efficiency (BFE)

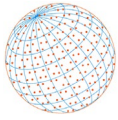
According to the EN14683:2019+AC standard, a sample of the MFM material is clamped between a viable six-stage cascade impactor and an aerosol chamber. A *Staphylococcus aureus* aerosol is generated into the aerosol chamber and sampled by the cascade impactor downstream of the tested MFM material. The experimental setup used by Lab.3 and Lab.4 are presented in Fig. 3.

The BFE is indicated by the colony forming units (CFU) counts that pass through the MFM. Each sample must measure at least 100 mm × 100 mm and must consist of all layers of the mask, in the same order as the finished mask. Prior to testing, each sample should be conditioned for at least 4 h to reach equilibrium in an atmosphere at (21 ± 5)°C, the relative humidity being (85 ± 5)%. The mean particles size (MPS) of the bacteriological aerosol must be maintained at 3.0 μm ± 0.3 μm. MPS value is calculated for each stage of the cascade impactor and is calculated as:

$$MPS = \frac{\sum(P_x \cdot C_x)}{\sum C_x} \quad (3)$$

where P_x is the 50% effective cut-off diameters of each of the six stages and C_x is the viable particle counts obtained from each of the six agar collection surfaces ($x = 1-6$). The EN 14683 thus imposes only two specifications for the choice of bioaerosol nebulizer: a MPS of 3.0 ± 0.3 μm and 1700–3000 CFUs of bacteria per test.

A first positive control is carried out by nebulizing the biological aerosol without the tested MFM sample. The BFE is therefore characterized by using a second step in which the MFM sample is introduced at the inlet of the cascade impactor. At each stage of the viable cascade impactor, the Petri dishes are exposed to the bacteriological aerosol. This second step is repeated at least five times and an additional positive control process is performed. Finally, a negative control process is carried out without the biological aerosol, i.e., by sampling air only into the viable cascade impactor. After incubation of the petri dishes at (37 ± 2)°C for 20 hours to 52 hours, CFU counts are performed for each sample and control process on each dish. Results are therefore summed to obtain the total CFU number. For each sample, the BFE is calculated using the following formula:



$$BFE = \frac{C - T}{C \times 100} \quad (4)$$

where C is the mean of the two positive controls of the total of the six stages, and T is the total of the six stages counts for each test sample. In the EN 14683 standard, filtration velocity is not mentioned. Nevertheless, by knowing the flow rate of 28.3 L min^{-1} and the effective filtration surface of 46.5 cm^2 intrinsic to the cascade impactor inlet, a filtration velocity of 10.1 cm s^{-1} can be calculated and will be used for proceeding to equivalent measurement between BFE and PFE.

2.2.1 Lab.3 experimental set-up

BFE experiments have been performed in a class II biosafety cabinet. The length of the aerosol chamber has been reduced compared to the EN 14683:2019 standard without changing the features of the bioaerosol arriving. *Staphylococcus aureus* (ATCC 6538) was inoculated into 30 mL of tryptic soy broth in a 50 mL flask and incubated with gentle shaking at $37 \pm 2^\circ\text{C}$ for 24 ± 2 hours.

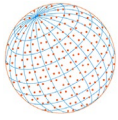
BFE testing has been done for decades using jet nebulizers (like the collision jet). Nevertheless, a modern vibrating mesh nebulizer has been used in recent studies of bioaerosol generation. Here, the E-Flow® mesh nebulizer (Pari GmbH, Starnberg, Germany) was used to aerosolize $3.0 \pm 0.3 \mu\text{m}$ droplets from a 3 mL suspension with 3000 CFU mL^{-1} of *S. aureus*. A bacterial challenge of 1700 to 3000 CFU per test has been used for 1 min of nebulization. The airflow was sent through the cascade impactor for an additional minute. The test therefore lasted for a total of 2 minutes. Petri dishes were removed from the viable cascade impactor (ACI) and incubated at $37 \pm 2^\circ\text{C}$ for 22 ± 2 hours. Colonies were counted with an automatic HD colony counter (Scan® 1200, Intersciences, France) or with a visual count of positive holes, after conversion into viable particles.

The cascade impactor used is the six-stage viable ACI (Tisch Environmental, Cleves, OH, USA). It contains several orifices requiring an exact flow of 28.3 L min^{-1} , generated using a vacuum pump. A single stage of this impactor contains up to 400 precision machine jet orifices. Their size is between 1.81 mm on the first stage and 0.25 mm on the sixth stage. The particles collected at each stage have size ranges depending on the velocity of the jet at this stage and the cut-off of the previous one. The 50% effective cut-off diameters for each of the six stages operating at 28.3 L min^{-1} are $7 \mu\text{m}$ for stage 1 (1.81 mm holes), $4.7 \mu\text{m}$, $3.3 \mu\text{m}$, $2.1 \mu\text{m}$, $1.1 \mu\text{m}$ and $0.65 \mu\text{m}$ for stage 6 (0.25 mm holes). Size-selective particle sampling with an impactor is based on the aerodynamic equivalent diameter, which takes into consideration the geometric particle size, shape and density. In this particle size range, the aerodynamic diameter is also the relevant diameter that describes the deposition of particles in the different regions of the human lung. Airborne bacteria are directly deposited on Petri dishes, positioned inside the cascade impactor. 100-mm glass Petri dishes have been substituted with 90-mm plastic Petri dishes inside the ACI. In comparison to the experimental setup shown in Fig. 3, the condenser in the Lab. 3 set-up was replaced by a filter and the flow rate was measured at the impactor inlet before the test. The uncertainties associated with Lab. 3 BFE measurements are calculated as standard deviation from the five tests.

2.2.2 Lab.4 experimental set-up

The experimental test bench used by Lab.4 was similar to the one presented in Fig. 3. All tests were carried out in a Biosafety Level 2 (BSL2) laboratory. The test preparation involves a calibrated *Staphylococcus aureus* suspension whose concentration is verified with a spectrophotometer using a 630 nm wavelength. The bacterial concentration was determined and adjusted, in order to reach a final concentration between 1.7×10^3 and 3.0×10^3 UFC per test. The prepared inoculum was injected by a syringe pump (Model: NE-300 « Jus infusion TM ») in the nebuliser to be released by activating a vacuum pump in the cascade impactor for 1 minute (flow rate = 28.3 L min^{-1}). A HEPA H14 filter was present upstream of the nebulizer column to prevent the spread of *Staphylococcus aureus* in the air. The airflow was maintained in the cascade impactor for an additional minute by stopping the nebuliser only. The generated inoculum was collected via a multi-orifice cascade impactor characterized by the same cut-off diameters as previously described.

The sterilized petri dishes were made of glass and consist of a 27mL growth medium (trypticase soy). The CFUs per dish are also counted by a colony counter (Scan® 1200). The number of viable particles in the sample was not equal to the number of bacterial cells in the sample, because one



viable particle can contain more than one cell. The result was obtained by counting and correlation to a conversion table which meets the “positive-hole” method. The conversion table used is based on the principle whereby the more the number of viable particles impacted on a Petri dish increases, the more the likelihood of the next one entering a positive hole decreases. The measurement uncertainties were based on the documentation provided by the manufacturer of the various components, the cascade impactor and the colony counter used for enumeration.

3 RESULTS

3.1 Filtration Efficiencies Comparison

Results of PFE and BFE measurements are compared in Fig. 4 for the 6 involved MFM samples. Each graph shows the result for one MFM sample, and each point a measurement for each laboratory. White areas show the Type II filtration efficiencies ($\geq 98\%$), light gray area the Type I (between 95 and 98%), and dark gray area the filtration efficiencies that are below 95%.

This figure shows that, for 3 μm -PFE measurements, the results for sample 1, 2, 3 and 5 are in very good agreement and are in the same range of filtration efficiency, which therefore characterize the MFM type. A maximum deviation of 4% is observed for sample 2. The values with their uncertainties are comprised within a 27% range, which is in good agreement with the previous study of Bourrous *et al.* (2021) about a 3 μm -PFE interlaboratory comparison on community face covering using a filtration velocity of 6 cm s^{-1} . The observed dispersion of 27% might be due to (i) the heterogeneity of the test media, to (ii) complex experimental procedures and devices (mainly the APS TSI 3321 used by Lab.1 and Lab.2) used to determine the PFE (Pfeifer *et al.*, 2016) and to (iii) the solid or liquid test aerosols. Identified experimental error sources are also the aerosol number concentration stability, the aerosol sampling devices and the APS counting efficiency (Armendariz and Leith, 2002; Volckens and Peters, 2005). This agreement also validates measurement protocols used by Lab. 1 and Lab. 2, for monodisperse (Lab. 1) and polydisperse (Lab. 2) aerosols. These 3 μm -PFE measurements have been then compared to BFE measurements.

For sample 4 and 6, the MFM are characterized by 3 μm -PFE $> 95\%$ associated to Type I for Lab. 1 and Type II for Lab. 2 with a difference of less than 3.5% between both labs.

For BFE measurements, the results are in good agreement for sample 1 and 5. Both of these samples are therefore determined to be Type II, as for 3 μm -PFE measurements. For sample 2,

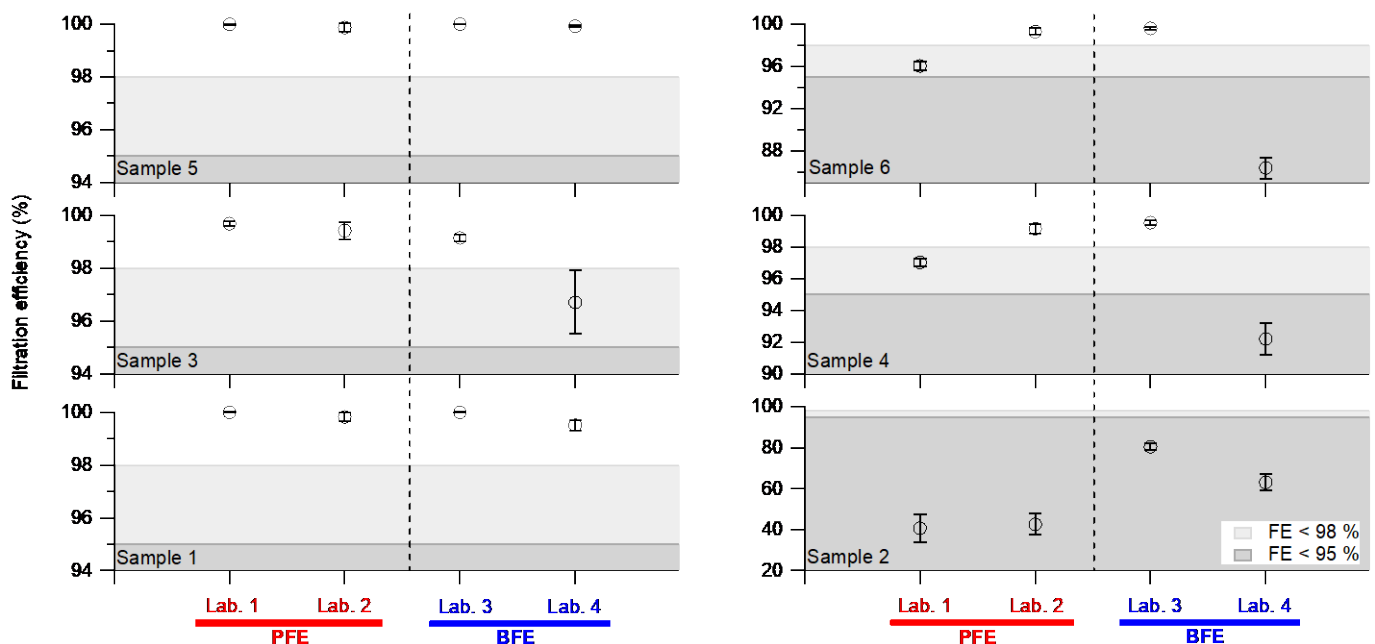
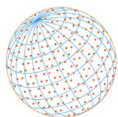


Fig. 4. Inter-laboratory comparison of 3 μm -PFE measured by Lab. 1 and 2 (PFE, underlined in red) vs. BFE measured by Lab. 3 and Lab. 4 (BFE, underline in blue) using a filtration velocity of 10.1 cm s^{-1} .



despite a difference of 22% between two BFE measurements, both of the laboratories find it non-compatible, i.e., BFE less than 95%. Finally, Lab. 3 and 4 are in less good agreement for samples 3, 4 and 6, classing them in different types, with relative differences of 2%, 7% and 13% respectively. Globally, the results are in good agreement between PFE and Lab. 3. For sample 2, all the laboratories find the associated MFM not compatible with Type I and II. For sample 3, the maximum difference between all the filtration efficiency results is 3%, but Lab. 4 results indicate a Type I classification with BFE less than 95%. For samples 4 and 6, the agreement is less good, with a high level of dispersion.

Then, in a certification scenario of these MFM, the classification of a same sample would not be in the same Type, except for samples 1, 2 and 5. The most problematic case would be for sample 4 and 6, which are not satisfying for Lab. 4 and characterized as Type II for Lab. 2 and Lab. 3. As a reminder, BFE is calculated for all the impactor stages and not only for the 3 μm stage (which correspond to stage 4 in the cascade impactor) in order to reach a comparison with 3 μm -PFE. This can therefore generate a bias in this comparison. To better understand and explain the differences observed between BFE and 3 μm -PFE, fractional efficiencies have been measured for Lab.2, Lab.3 and Lab.4 and need to be plotted to compare stage 4 efficiencies to 3 μm -PFE.

3.2 Fractional Efficiency

For each MFM sample, Fig. 5 shows fractional efficiencies (SE), which are filtration efficiencies calculated for different aerodynamic diameters of test aerosols. As previously, each graph shows the measurement realized for one sample and each plot shows one laboratory SE, except for Lab. 1, which did not proceed to any fractional determination due to the use of 3 μm PSL as a monodisperse aerosol. The filtration efficiency at 3 μm measured by Lab. 1 is shown with black squares. For Lab. 3 and Lab. 4, the BFE calculated for each stage of the cascade impactor are shown, between 0.65 μm (cut-off diameter of stage 1) and 7 μm (cut-off diameter of stage 6). As a reminder, stage 3 and 4 corresponds to cut-off sizes of 3.3 and 2.1 respectively. By taking into

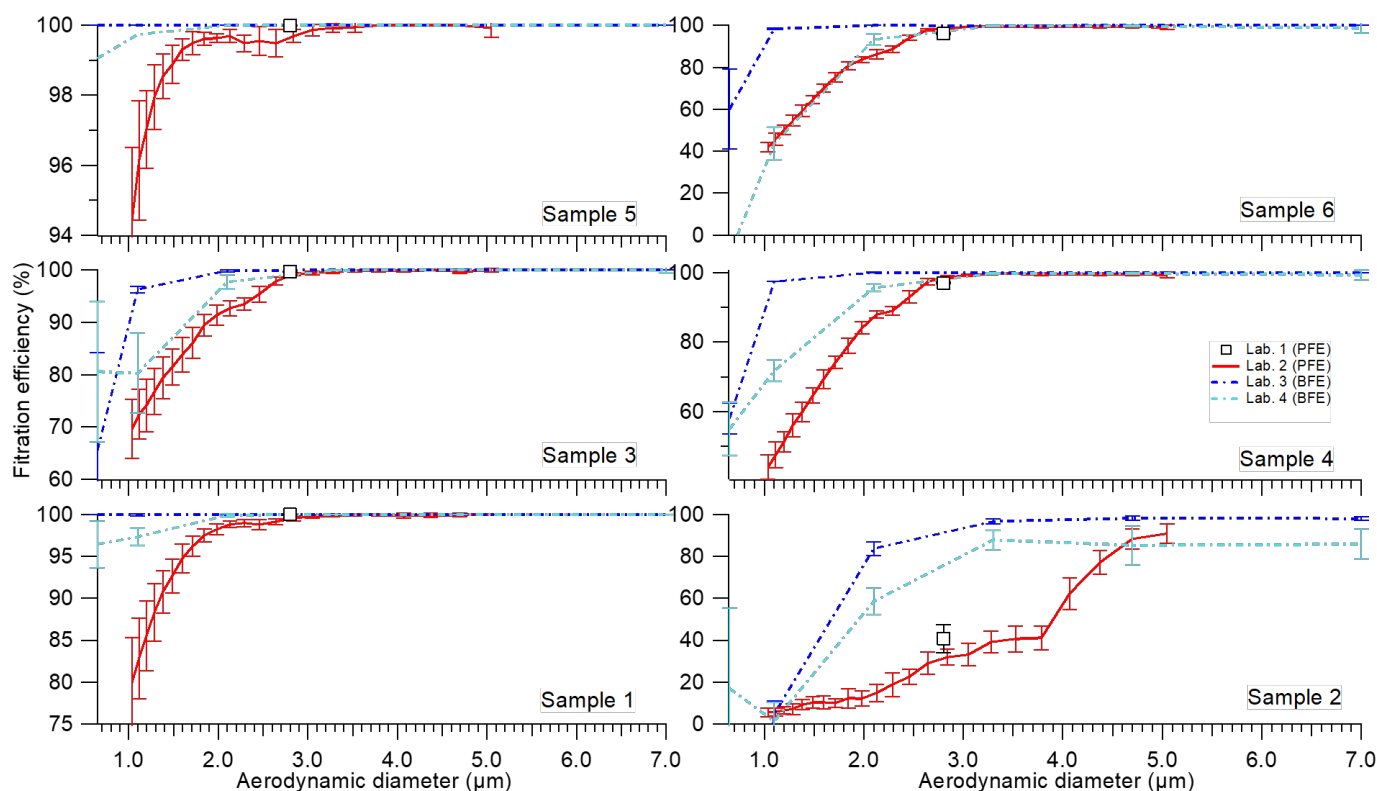


Fig. 5. Fractional filtration (SE) efficiency of each MFM sample measured by Lab. 2 using PFE method (red line), and by Lab. 3 and Lab. 4 (blue and green lines respectively) using BFE method. The filtration efficiency at 3 μm measured by Lab. 1 is shown with black squares.

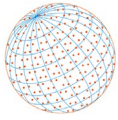


Table 1. Relative deviations of Lab. 3 and 4 BFE measurements in comparison to the average 3 μm -PFE measurements.

Sample	Lab. 3		Lab. 4	
	$\left \frac{\overline{\text{PFE}} - \text{BFE}}{\overline{\text{PFE}}} \right $	$\left \frac{\overline{\text{PFE}} - \text{BFE}_{\text{stage 4}}}{\overline{\text{PFE}}} \right $	$\left \frac{\overline{\text{PFE}} - \text{BFE}}{\overline{\text{PFE}}} \right $	$\left \frac{\overline{\text{PFE}} - \text{BFE}_{\text{stage 4}}}{\overline{\text{PFE}}} \right $
	PFE	PFE	PFE	PFE
1	0.1%	0.1%	0.4%	0.1%
2	93.3%	132.0%	51.6%	110.9%
3	0.4%	0.5%	2.9%	0.4%
4	1.5%	1.9%	6.0%	1.7%
5	0.1%	0.1%	0.1%	0.1%
6	2.0%	2.3%	11.5%	2.2%

account steep impaction curves, 3 μm particles are mainly collected on stage 4. Therefore, 3 μm -PFE results were compared to this stage 4. For Lab. 2, SE have been measured between 1 μm and 5 μm .

For samples 1, 3, 4, 5 and 6, Fig. 5 shows that SE measurements diverge for aerodynamic diameter smaller than 3 μm , in link with a filtration efficiency decreasing associated with the typical U-shape of the SE. For aerodynamic diameter below 3 μm , BFE measurements are generally higher than 3 μm -PFE measurement, except for sample 6, for which Lab. 2 (3 μm -PFE) and Lab. 4 (BFE) measurements are very close. Then, a good agreement is shown between 3 μm -PFE (black squares) and stage 4 BFE. For higher values of aerodynamic diameter, filtration efficiencies tend to 100% and agree between all laboratories. Sample 2 appears to be an exception. Fractional efficiencies seem to diverge in all the diameter range. A possible explanation could be a biocidal treatment, potentially applied to all samples involved in this study, but enhanced for sample 2 due to its low filtration efficiency. Indeed, such a biocidal process could have an effect on bacteria and not on inert particles. A common tendency is shown by BFE measurements, but Lab. 4 values are lower compare to Lab. 3. At 3 μm , BFE values are higher than 3 μm -PFE. However, it is important to mention that all laboratories find filtration efficiencies at 3 μm lower than 95%, leading to a non-validation of this MFM sample for Type I or Type II classification. Table 1 shows the relative deviations between the average 3 μm -PFE results calculated for each sample from Lab. 1 and Lab. 2 measurements, and BFE measurements performed by Lab. 3 and Lab. 4. A comparison is also presented with BFE measurements obtained at the stage 4 ($\text{BFE}_{\text{stage4}}$) of the cascade impactor only.

These results confirm that Lab. 3 measurements are in good agreement with 3 μm -PFE for all the samples, except for sample 2. The use of stage 4 does not improve the agreement, which is almost constant for most of the samples. For Lab. 4, $\text{BFE}_{\text{stage4}}$ measurements lead to a major decrease of deviations in comparison to 3 μm -PFE, and appears to be similar to Lab. 3. This shows the potential bias of BFE measurement for Lab.4 from the EN 14683 protocol which involves the use of a BFE mean value calculated from all the cascade impactor stages. However, an opposite behavior is shown for sample 2. Indeed, the $\text{BFE}_{\text{stage4}}$ deviation is higher than the BFE. This can be explained by the fact that the BFE measurements for the sample 2 are lower compared to $\text{BFE}_{\text{stage4}}$ measurements for both Labs.

4 DISCUSSION AND OUTLOOK

In this work, several hypotheses have been considered to explain the observed differences between 3 μm -PFE and BFE measurements. First, there might be a heterogeneity of the test media. Each MFM sample can indeed present small manufacturing differences, which can induce variability in terms of filtration efficiencies. Nevertheless, for MFM characterized with high performances, this is expected to be negligible. This might be an important cause for differences in sample 2 filtration efficiency measurements for example.

Secondly, it can also be linked to the biological aerosol during BFE measurements, particularly through two phenomena, i.e., droplets degradation and bacteria deaths when passing through the MFM sample. The prior can lead to a shift of the size distribution towards smaller diameter,



and thus to underestimated filtration efficiencies at the associated stages of the cascade impactor. The latter might lead to a decrease of CFU counts, and then to a BFE overestimation. Also, several questions are raised by the simplicity of this test. The air jets of the cascade impactor directly impinge onto a Petri dish nutrient, which is then incubated until the formation of colonies of collected bacteria. However, this can affect the resulting CFU counts accuracy obtained from Petri dishes. Indeed, the CFU counts can be adjusted by the likelihood that one bacterium can be merged with another at an impaction site to produce a single colony. Macher, 1989 proposed a “positive-hole” correction table allowing for the correction of the cascade impactors positive-hole visual counts. However, this method appears to be time-consuming and operator-dependent, and visual counting might be a source of bias. A new method involving direct colony counting using high-resolution automatic color colony counters allows a more accurate and reproducible CFU counting on Petri dishes, and no correction seems to be required (Pourchez *et al.*, 2021).

Thirdly, as a reminder, it is important to point out that the BFE is calculated globally on the basis of CFU counts from all cascade impactor stages and corresponding to a wide range of particle cut-off diameters, without being specific to the stage corresponding to the “average size of 3 μm ”.

Moreover, differences between BFE measurements can be explained by the generations of the biological aerosol. E-Flow® mesh nebulizer (Pari GmbH, Starnberg, Germany) and 4-jets Blaustein Atomizing Modules (BLAM) were used by Lab. 3 and Lab. 4, respectively. Both generators produce aerosols using different technical parameters, such as liquid sample volumes, and this leads to the generation of polydisperse aerosols characterized by a broad size range in terms of aerodynamic diameters, i.e., delivering particles with a mean size of $3.0 \pm 0.3 \mu\text{m}$, but associated with different size distributions. This can explain deviations between BFE measurements themselves, since BFE is calculated as a mean value of all the stages of the cascade impactor. If the amount of small size droplets ($< 3 \mu\text{m}$ in terms of aerodynamic diameter) is higher, this will have a direct impact on fractional efficiencies and therefore to the mean BFE value which will be lower. A need is highlighted for such a nebulization process in terms of particle number size distribution characterization and not only in terms of average size characterization.

Another point concerns the fast water saturation of the MFM sample at the beginning of a BFE experiment, causing a modification in terms of filtration velocity and therefore in terms of characterization of the associated BFE fractional efficiency used for the global BFE calculation. However, the EN 14683 standard specifies conditioning of the media to be tested in terms of temperature and relative humidity before the tests. The usefulness of this conditioning is therefore debatable in link with previous comment. In this context of environmental conditions in terms of relative humidity and temperature, particle size can change inside the impactor due to water evaporation/condensation. This is a well-studied bias of cascading impactors. Indeed, previous studies investigated the temperature effect on aerosol size by impactor cooling in order to limit droplet evaporation (Stapleton and Finlay, 1998; Kwong *et al.*, 2000; Zhou *et al.*, 2005a; Rao *et al.*, 2010). Other studies also investigated the humidity effect on particle size distribution measurements (Prokop *et al.*, 1995; Finlay *et al.*, 1997; Nerbrink *et al.*, 2003; Zhou *et al.*, 2005b). However, aerosols with large numbers of droplets per unit volume, which is the case of this study, can actually self-humidify the surrounding air and therefore stop the size changes (Majoral *et al.*, 2020). This phenomenon occurs when the number of droplets is high, i.e., the vapor evaporating off the droplets implies the air to reach water vapor equilibrium (Finlay and Smaldone, 1998). Moreover, it is important to mention that no sample volume to be generated is specified within this standard, nor filtration velocity since no precise effective filtration surface is given. Overall, it is legitimate to ask the question of characterizing MFM filtration efficiencies in terms of (i) $\text{BFE}_{\text{stage4}}$, (ii) 3 μm -PFE or (iii) PFE, rather than in terms of BFE (Whyte *et al.*, 2022).

5 CONCLUSION

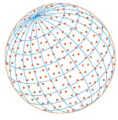
In connection with the COVID-19 pandemic, and the need for characterizing the performance of MFM and in terms of filtration efficiency, an interlaboratory comparison has been conducted. The aim of this study was to compare, for a given medium, the results in terms of particular filtration efficiency (PFE) and bacterial filtration efficiency (BFE). To do this, a uniform filtration velocity of 10.1 cm s^{-1} was adopted by all the participants in accordance with the normative context



(EN 14683, flow rate of 28.3 L min^{-1} and effective filtration area of 46.5 cm^2). A good agreement between the PFE measurements but a disagreement between the BFE measurements are shown. A greater scatter of filtration efficiency results was also obtained for media with non-compliant BFE. Regarding the normative context associated with surgical masks (EN14683:2019+AC), it should be noted that the use of a bio-aerosol can lead to many questions, in particular concerning the risk of loss of bacteria. In addition, the EN 14683 standard specifies the use of a nebulizer capable of generating particles with an average size of $3.0 \pm 0.3 \mu\text{m}$. However, such a nebulization process can be characterized by the generation of a polydisperse aerosol having a different particle size distributions in number but corresponding to such an average size. In addition, note that the BFE is calculated globally on the basis of a count of Colony Forming Units (CFU) obtained on all the stages of a cascade impactor and corresponding to a wide range of particle cut-off diameters, without being specific to the stage corresponding to the “average size of $3 \mu\text{m}$ ”. No filtration velocity is also specified within this standard, nor the volume of liquid sample to be generated in aerosol phase, nor the generation time. This document also specifies conditioning of the media to be tested in terms of temperature and relative humidity before the tests. But, given the very rapid water saturation from the first minute of the tests involving the conditioned media, this conditioning step does not seem really necessary.

REFERENCES

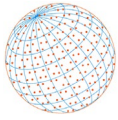
- Armendariz, A.J., Leith, D. (2002). Concentration measurement and counting efficiency for the aerodynamic particle sizer 3320. *J. Aerosol Sci.* 33, 133–148. [https://doi.org/10.1016/S0021-8502\(01\)00152-5](https://doi.org/10.1016/S0021-8502(01)00152-5)
- Asadi, S., Bouvier, N., Wexler, A.S., Ristenpart, W.D. (2020a). The coronavirus pandemic and aerosols: Does COVID-19 transmit via expiratory particles? *Aerosol Sci. Technol.* 54, 635–638. <https://doi.org/10.1080/02786826.2020.1749229>
- Asadi, S., Cappa, C.D., Barreda, S., Wexler, A.S., Bouvier, N.M., Ristenpart, W.D. (2020b). Efficacy of masks and face coverings in controlling outward aerosol particle emission from expiratory activities. *Sci. Rep.* 10, 15665. <https://doi.org/10.1038/s41598-020-72798-7>
- ASTM International (2019). ASTM F2100-19. Standard Specification for Performance of Materials Used in Medical Face Masks. ASTM International, West Conshohocken, PA.
- Bahl, P., Doolan, C., de Silva, C., Chughtai, A.A., Bourouiba, L., MacIntyre, C.R. (2020). Airborne or droplet precautions for health workers treating coronavirus disease 2019? *J. Infect. Dis.* 225, 1561–1568. <https://doi.org/10.1093/infdis/jiaa189>
- Birgand, G., Peiffer-Smadja, N., Fournier, S., Kerneis, S., Lescure, F.X., Lucet, J.C. (2020). Assessment of air contamination by SARS-CoV-2 in hospital settings. *JAMA Netw. Open* 3, e2033232–e2033232. <https://doi.org/10.1001/jamanetworkopen.2020.33232>
- Bourouiba, L. (2020). Turbulent gas clouds and respiratory pathogen emissions: Potential implications for reducing transmission of COVID-19. *JAMA* 323, 1837–1838. <https://doi.org/10.1001/jama.2020.4756>
- Bourrous, S., Barrault, M., Mocho, V., Poirier, S., Bardin-Monnier, N., Charvet, A., Thomas, D., Bescond, A., Fouqueau, A., Mace, T., Gaie-Levrel, F., Ouf, F. (2021). A performance evaluation and inter-laboratory comparison of community face coverings media in the context of COVID-19 pandemic. *Aerosol Air Qual. Res.* 21, 200615. <https://doi.org/10.4209/aaqr.200615>
- Chen, S.K., Vesley, D., Brosseau, L.M., Vincent, J.H. (1994). Evaluation of single-use masks and respirators for protection of health care workers against mycobacterial aerosols. *Am. J. Infect. Control* 22, 65–74. [https://doi.org/10.1016/0196-6553\(94\)90116-3](https://doi.org/10.1016/0196-6553(94)90116-3)
- Cheng, V.C.C., Wong, S.C., Chen, J.H.K., Yip, C.C.Y., Chuang, V.W.M., Tsang, O.T.Y., Sridhar, S., Chan, J.F.W., Ho, P.L., Yuen, K.Y. (2020a). Escalating infection control response to the rapidly evolving epidemiology of the coronavirus disease 2019 (COVID-19) due to SARS-CoV-2 in Hong Kong. *Infect. Control Hosp. Epidemiol.* 41, 493–498. <https://doi.org/10.1017/ice.2020.58>
- Cheng, Y., Ma, N., Witt, C., Rapp, S., Wild, P., Andreae, M.O., Pöschl, U., Su, H. (2020b). Distinct regimes of particle and virus abundance explain face mask efficacy for COVID-19. *medRxiv* 2020.09.10.20190348. <https://doi.org/10.1101/2020.09.10.20190348>
- Chia, P.Y., Coleman, K.K., Tan, Y.K., Ong, S.W.X., Gum, M., Lau, S.K., Lim, X.F., Lim, A.S., Sutjipto,



- S., Lee, P.H., Son, T.T., Young, B.E., Milton, D.K., Gray, G.C., Schuster, S., Barkham, T., De, P.P., Vasoo, S., Chan, M., Ang, B.S.P., *et al.* (2020). Detection of air and surface contamination by SARS-CoV-2 in hospital rooms of infected patients. *Nat. Commun.* 11, 2800. <https://doi.org/10.1038/s41467-020-16670-2>
- Dancer, S.J., Tang, J.W., Marr, L.C., Miller, S., Morawska, L., Jimenez, J.L. (2020). Putting a balance on the aerosolization debate around SARS-CoV-2. *J. Hosp. Infect.* 105, 569–570. <https://doi.org/10.1016/j.jhin.2020.05.014>
- Eiche, T., Kuster, M. (2020). Aerosol release by healthy people during speaking: Possible contribution to the transmission of SARS-CoV-2. *Int. J. Environ. Res. Public Health* 17, 9088. <https://doi.org/10.3390/ijerph17239088>
- European Committee for Standardization (CEN) (2009). EN149+A1. Respiratory protective devices Filtering half masks to protect against particles Requirements, testing, marking. CEN, Brussels.
- European Committee for Standardization (CEN) (2019a). EN13274-7. Respiratory protective devices - Methods of test - Part 7: determination of particle filter penetration. CEN, Brussels.
- European Committee for Standardization (CEN) (2019b). EN14683+AC. Medical face masks - Requirements and test methods. CEN, Brussels.
- Faridi, S., Niazi, S., Sadeghi, K., Naddafi, K., Yavarian, J., Shamsipour, M., Jandaghi, N.Z.S., Sadeghniaat, K., Nabizadeh, R., Yunesian, M., Momeniha, F., Mokamel, A., Hassanvand, M.S., MokhtariAzad, T. (2020). A field indoor air measurement of SARS-CoV-2 in the patient rooms of the largest hospital in Iran. *Sci. Total Environ.* 725, 138401. <https://doi.org/10.1016/j.scitotenv.2020.138401>
- Finlay, W.H., Stapleton, K.W., Zuberbuhler, P. (1997). Errors in regional lung deposition predictions of nebulized salbutamol sulphate due to neglect or partial inclusion of hygroscopic effects. *Int. J. Pharm.* 149, 63–72. [https://doi.org/10.1016/S0378-5173\(96\)04860-0](https://doi.org/10.1016/S0378-5173(96)04860-0)
- Finlay, W.H., Smaldone, G.C. (1998). Hygroscopic behaviour of nebulized aerosols: Not as important as we thought? *J. Aerosol Med.* 11, 193–195. <https://doi.org/10.1089/jam.1998.11.193>
- Galbadage, T., Peterson, B.M., Gunasekera, R.S. (2020). Does COVID-19 spread through droplets alone? *Front. Public Health* 8, 163. <https://doi.org/10.3389/fpubh.2020.00163>
- Guo, Z.D., Wang, Z.Y., Zhang, S.F., Li, X., Li, L., Li, C., Cui, Y., Fu, R.B., Dong, Y.Z., Chi, X.Y., Zhang, M.Y., Liu, K., Cao, C., Liu, B., Zhang, K., Gao, Y.W., Lu, B., Chen, W. (2020). Aerosol and surface distribution of Severe Acute Respiratory Syndrome Coronavirus 2 in hospital wards, Wuhan, China, 2020. *Emerg. Infect. Dis.* 26, 1583–1591. <https://doi.org/10.3201/eid2607.200885>
- Hobday, R.A., Dancer, S.J. (2013). Roles of sunlight and natural ventilation for controlling infection: Historical and current perspectives. *J. Hosp. Infect.* 84, 271–282. <https://doi.org/10.1016/j.jhin.2013.04.011>
- Johnson, G.R., Morawska, L., Ristovski, Z.D., Hargreaves, M., Mengersen, K., Chao, C.Y.H., Wan, M.P., Li, Y., Xie, X., Katoshevski, D., Corbett, S. (2011). Modality of human expired aerosol size distributions. *J. Aerosol Sci.* 42, 839–851. <https://doi.org/10.1016/j.jaerosci.2011.07.009>
- Jones, R.M., Brosseau, L.M. (2015). Aerosol transmission of infectious disease. *J. Occup. Environ. Med.* 57, 501–508. <https://doi.org/10.1097/JOM.0000000000000448>
- Kwong, W.T.J., Ho, S.L., Coates, A.L. (2000). Comparison of nebulized particle size distribution with Malvern laser diffraction analyzer versus Andersen cascade impactor and low-flow Marple personal cascade impactor. *J. Aerosol Med.* 13, 303–314. <https://doi.org/10.1089/jam.2000.13.303>
- Leung, N.H.L., Chu, D.K.W., Shiu, E.Y.C., Chan, K.H., McDevitt, J.J., Hau, B.J.P., Yen, H.L., Li, Y., Ip, D.K.M., Peiris, J.S.M., Seto, W.H., Leung, G.M., Milton, D.K., Cowling, B.J. (2020). Respiratory virus shedding in exhaled breath and efficacy of face masks. *Nat. Med.* 26, 676–680. <https://doi.org/10.1038/s41591-020-0843-2>
- Liu, Y., Ning, Z., Chen, Y., Guo, M., Liu, Y., Galí, N.K., Sun, L., Duan, Y., Cai, J., Westerdahl, D., Liu, X., Xu, K., Ho, K., Kan, H., Fu, Q., Lan, K. (2020). Aerodynamic analysis of SARS-CoV-2 in two Wuhan hospitals. *Nature* 582, 557–560. <https://doi.org/10.1038/s41586-020-2271-3>
- Majoral, C., Coates, A.L., Le Pape, A., Vecellio, L. (2020). Humidified and heated cascade impactor for aerosol sizing. *Front. Bioeng. Biotechnol.* 8, 589782. <https://doi.org/10.3389/fbioe.2020.589782>
- McCullough, N.V., Brosseau, L.M., Vesley, D. (1997). Collection of three bacterial aerosols by respirator and surgical mask filters under varying conditions of flow and relative humidity. *Ann.*



- Occup. Hyg. 41, 677–690. [https://doi.org/10.1016/S0003-4878\(97\)00022-7](https://doi.org/10.1016/S0003-4878(97)00022-7)
- Milton, D.K., Fabian, M.P., Cowling, B.J., Grantham, M.L., McDevitt, J.J. (2013). Influenza virus aerosols in human exhaled breath: Particle size, culturability, and effect of surgical masks. *PLoS Pathogens* 9, e1003205. <https://doi.org/10.1371/journal.ppat.1003205>
- National Standards Authority of Ireland (NSAI) (2020). S.R. CWA 17553:2020. Community face coverings - Guide to minimum requirements, methods of testing and use. NSAI, Ireland. https://www.n sai.ie/images/uploads/standards/SR_CWA17553_2020.pdf
- Nerbrink, O.L., Pagels, J., Pieron, C.A., Dennis, J.H. (2003). Effect of humidity on constant output and breath enhanced nebulizer designs when tested in the EN13544-1 EC Standard. *Aerosol Sci. Technol.* 37, 282–292. <https://doi.org/10.1080/027868203000948>
- Ng, C.S., Chong, K.L., Yang, R., Li, M., Verzicco, R., Lohse, D. (2021). Growth of respiratory droplets in cold and humid air. *Phys. Rev. Fluids* 6, 054303. <https://doi.org/10.1103/PhysRevFluids.6.054303>
- Nicas, M., Nazaroff, W.W., Hubbard, A. (2005). Toward understanding the risk of secondary airborne infection: Emission of respirable pathogens. *J. Occup. Environ. Hyg.* 2, 143–154. <https://doi.org/10.1080/15459620590918466>
- Ong, S.W.X., Tan, Y.K., Chia, P.Y., Lee, T.H., Ng, O.T., Wong, M.S.Y., Marimuthu, K. (2020). Air, surface environmental, and personal protective equipment contamination by severe acute respiratory syndrome coronavirus 2 (SARS-CoV-2) from a symptomatic patient. *JAMA* 323, 1610–1612. <https://doi.org/10.1001/jama.2020.3227>
- Peters, A., Parneix, P., Otter, J., Pittet, D. (2020). Putting some context to the aerosolization debate around SARS-CoV-2. *J. Hosp. Infect.* 105, 381–382. <https://doi.org/10.1016/j.jhin.2020.04.040>
- Pfeifer, S., Müller, T., Weinhold, K., Zikova, N., Dos Santos, S.M., Marinoni, A., Bischof, O.F., Kykal, C., Ries, L., Meinhardt, F., Aalto, P., Mihalopoulos, N., Wiedensohler, A. (2016). Intercomparison of 15 aerodynamic particle size spectrometers (APS 3321): Uncertainties in particle sizing and number size distribution. *Atmos. Meas. Tech.* 9, 1545–1551. <https://doi.org/10.5194/amt-9-1545-2016>
- Pourchez, J., Peyron, A., Montigaud, Y., Laurent, C., Audoux, E., Leclerc, L., Verhoeven, P.O. (2021). New insights into the standard method of assessing bacterial filtration efficiency of medical face masks. *Sci. Rep.* 11, 5887. <https://doi.org/10.1038/s41598-021-85327-x>
- Prokop, R.M., Finlay, W.H., Stapleton, K.W., Zuberbuhler, P. (1995). The effect of ambient relative humidity on regional dosages delivered by a jet nebulizer. *J. Aerosol Med.* 8, 363–372. <https://doi.org/10.1089/jam.1995.8.363>
- Rao, N., Kadrichu, N., Ament, B. (2010). Application of a droplet evaporation model to aerodynamic size measurement of drug aerosols generated by a vibrating mesh nebulizer. *J. Aerosol Med. Pulm. Drug Deliv.* 23, 295–302. <https://doi.org/10.1089/jamp.2009.0805>
- Santarpia, J.L., Rivera, D.N., Herrera, V., Morwitzer, M.J., Creager, H., Santarpia, G.W., Crown, K.K., Brett-Major, D., Schnaubelt, E., Broadhurst, M.J., Lawler, J. V, Reid, St.P., Lowe, J.J. (2020). Aerosol and surface transmission potential of SARS-CoV-2. medRxiv 2020.03.23.20039446. <https://doi.org/10.1101/2020.03.23.20039446>
- Stapleton, K.W., Finlay, W.H. (1998). Errors in characterizing particle size distributions with cascade impactors. *J. Aerosol Med.* 11, S80–S83.
- Tellier, R., Li, Y., Cowling, B.J., Tang, J.W. (2019). Recognition of aerosol transmission of infectious agents: A commentary. *BMC Infect. Dis.* 19, 101. <https://doi.org/10.1186/s12879-019-3707-y>
- Volckens, J., Peters, T.M. (2005). Counting and particle transmission efficiency of the aerodynamic particle sizer. *J. Aerosol Sci.* 36, 1400–1408. <https://doi.org/10.1016/j.jaerosci.2005.03.009>
- Wang, H., Li, Z., Zhang, X., Zhu, L., Liu, Y., Wang, S. (2020). The motion of respiratory droplets produced by coughing. *Phys. Fluids* 32, 125102. <https://doi.org/10.1063/5.0033849>
- Weber, A., Willeke, K., Marchioni, R., Myojo, T., McKay, R., Donnelly, J., Liebhaber, F. (1993). Aerosol penetration and leakage characteristics of masks used in the health care industry. *Am. J. Infect. Control* 21, 167–173. [https://doi.org/10.1016/0196-6553\(93\)90027-2](https://doi.org/10.1016/0196-6553(93)90027-2)
- Whyte, H.E., Montigaud, Y., Audoux, E., Verhoeven, P., Prier, A., Leclerc, L., Sarry, G., Laurent, C., Le Coq, L., Joubert, A., Pourchez, J. (2022). Comparison of bacterial filtration efficiency vs. particle filtration efficiency to assess the performance of non-medical face masks. *Sci. Rep.* 12, 1188. <https://doi.org/10.1038/s41598-022-05245-4>



- Wong, S.C.Y., Kwong, R.T.S., Wu, T.C., Chan, J.W.M., Chu, M.Y., Lee, S.Y., Wong, H.Y., Lung, D.C. (2020). Risk of nosocomial transmission of coronavirus disease 2019: An experience in a general ward setting in Hong Kong. *J. Hosp. Infect.* 105, 119–127. <https://doi.org/10.1016/j.jhin.2020.03.036>
- World Health Organisation (WHO) (2020). Coronavirus: Events as they happen. World Health Organisation. <https://www.who.int/emergencies/diseases/novel-coronavirus-2019/events-as-they-happen>
- Worldometer (2022). Coronavirus Update (Live): Cases and Deaths from COVID-19 Virus Pandemic. Worldometers.
- Zhou, Y., Ahuja, A., Irvin, C.M., Kracko, D.A., McDonald, J.D., Cheng, Y.S. (2005a). Medical nebulizer performance: effects of cascade impactor temperature. *Respir. Care.* 50, 1077–1082.
- Zhou, Y., Ahuja, A., Irvin, C.M., Kracko, D., McDonald, J.D., Cheng, Y.S. (2005b). Evaluation of nebulizer performance under various humidity conditions. *J. Aerosol Med.* 18, 283–293. <https://doi.org/10.1089/jam.2005.18.283>